

# Chapter 12

## Application to Experiments

In the past three decades there have been a large number of papers reporting the experimental observation of chaos. In this chapter I describe two rather different classes of experiments.

First, some of the early experiments verifying the general idea that experimental systems show the phenomenon of chaos will be described. The emphasis is on “real” systems—ones that represent albeit simplified versions of phenomena in nature—rather than “artificial” ones such as electronic circuits or simple mechanical oscillators. It turns out the fluid systems are particularly convenient for precise, well controlled experiments, so a number of the examples are on various fluid experiments. The results are briefly described here—you are advised to read the original papers for the full story. Further experiments investigating various quantitative aspects of chaos, particularly the onset as a control parameter is increased, will be discussed later.

Chaotic phenomena also occur in the natural world, outside of the laboratory. One fascinating example is the role of chaos in heart arrhythmias. Obviously the heart in a living animal is a more complex system than a fluid experiment in the laboratory, and it is much harder to get clean experimental data. Nevertheless, there is growing evidence that spontaneous, deterministic chaotic dynamics is an important element in understanding the heart.

### 12.1 Demonstration Experiments

Although the study of fluid *turbulence* is an old area, the first experiments to suggest that the ideas of chaos were relevant to the development of turbulence as

the appropriate parameter is increased (here the Reynolds number) were probably those of Ahlers in 1974 [1] and Gollub and Swinney in 1975 [2].

The experiment by Ahlers was on Rayleigh-Bénard convection (c.f. the Lorenz model of chapter 1) in a horizontal cylindrical geometry of rather pancake shape (the radius was about 5 times the depth of the fluid). Since the convection roll is roughly circular in section, this meant that there were of order 10 rolls across the diameter, a number large enough to lead us now to expect rather complex “textures” of curved rolls with defects, rather than a simple pattern of straight convection rolls. For temperature differences across the cell larger than twice the value at which convection first onsets aperiodic time dependence was observed. (In this experiment the heat current through the cell was held constant, and the fluctuation temperature difference was measured.) The only diagnostics used was the power spectrum, which showed a broad band spectrum. The chaos developed from a time independent state, and from later experiments was probably due to the onset of dynamics in the defects (roll endings) within the cell.

Gollub and Swinney studied “Taylor-Couette” flow—the flow between two cylinders with the inner one rotated. This undergoes an instability rather analogous to the convection instability in which now the radial centrifugal forces drive circulating, azimuthal rolls above a critical rotation rate. Here the chaos developed from an oscillating state, and again the only diagnostics was the power spectrum.

Dubois and Bergé [4] studied the onset of chaos in a smaller, rectangular convection cell with only two convection rolls, and later [5] performed a reconstruction of the attractor using the Taken’s algorithm and measured the correlation dimension  $D_2$  at some point in the chaotic state, finding  $D_2 = 2.8$ .

A particularly nice reconstruction of a chaotic attractor was done for *chemical oscillations* by Roux et al. [6]. They found that a 3-dimensional phase space gave a good reconstruction of the attractor. They also found [7] that a one dimensional return map on the Poincaré section was well described by a function with a single smooth maximum, and that this could then give a detailed account of the sequence of chaotic and periodic states as a parameter was changed, corresponding to the rich set of states we studied in the quadratic map bifurcation diagram.

An interesting demonstration of the use of  $f(\alpha)$  is the comparison of the onset of chaos by the period doubling route [8], and through the break down of quasiperiodic motion [9]. As we will see quantitative predictions can be made at the onset of chaos in these two cases, including predictions for  $f(\alpha)$ . The experiments were on a small convection system (of about two rolls) using mercury as the fluid, with a magnetic field and a small oscillating electric current passed vertically through the fluid to provide a controlled periodic driving of the system.

Unfortunately, the ideas that seem most appropriate theoretically for defining chaos—a positive Lyapunov exponent or Kolmogorov entropy—are both rather difficult to obtain from experimental data. The Lyapunov exponents are hard to measure since the tangent space must be reconstructed by differencing data points that happen to come close together in the phase space reconstruction. An example is shown by Wolf et al. [10]. Similarly the Kolmogorov entropy  $K$  is hard to measure. Grassberger and Procaccia [11] introduced a quantity  $K_2$  related to  $K$  much as  $D_2$  is related to the capacity  $D_C$  that should be easier to measure. A recent numerical package that implements these ideas is the [Tisean](#) package described in reference [12].

## 12.2 Chaos in the Heart

According to the American Heart Association fibrillation in the ventricle of the heart is the dominant immediate cause of death in the industrialized world. Perhaps in as many as 1 in 25 of these deaths the sudden onset of fibrillation occurred in apparently healthy heart muscle (as opposed to muscle damaged by an infarct). There is growing evidence that fibrillation corresponds to chaotic motion of the muscle tissue. A non-fatal precursor condition, ventricular tachycardia, seems to correspond to the spontaneous formation of self-sustained spiral wave patterns in the muscle, so that the contraction of the heart is prompted by the “reentrant” wave propagation rather than by electrical pulses from the sinus node pace maker as in the normal behavior. Thus the heart provides a fascinating arena for the application of dynamical systems theory and chaos. The final story is certainly not in. The heart is a complicated, spatially heterogeneous structure in a time dependent environment. Furthermore, the “chaotic” fibrillation state is fatal if not corrected immediately, and so nontransient investigations must rely on studies of artificially maintained hearts outside of the body, which may not in fact have the same behavior as the *in vivo* heart. However ideas from the physical understanding of dynamical systems have already provided useful stimulus to experiments on actual hearts. In addition experimentalists are developing increasingly sophisticated tools for studying simplifications of the *in vivo* heart, for example rectangular slabs or rings of heart muscle with some (albeit presumably strongly perturbed) biological function remaining.

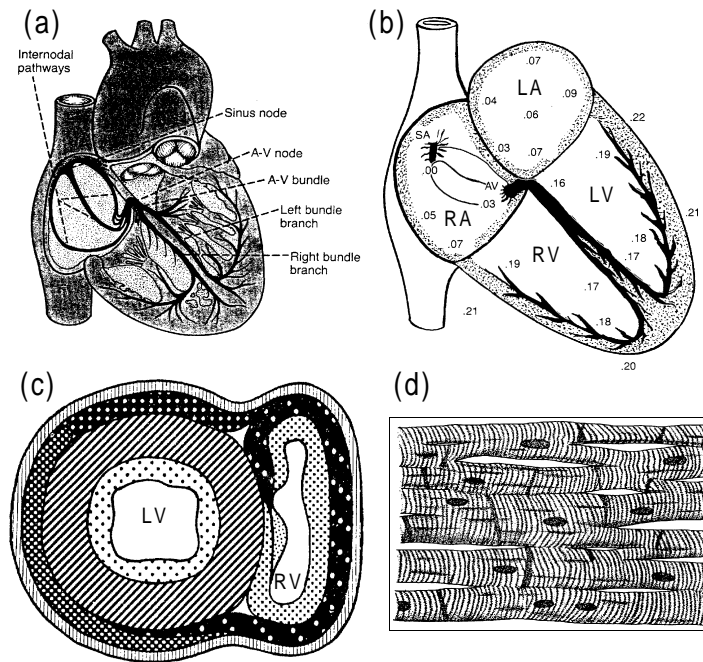


Figure 12.1: Electrophysiology of the heart: (a) sinus node and the Purkinje system; (b) transmission of cardiac pulse showing delay in fractions of a second in different parts of the heart (R,L right,left; A atrium; V ventricle); (c) Equatorial section of the heart; (d) Muscle fibres. [a,b, and d from ref. [13]; c from ref. [14]]

### 12.2.1 Physiology of the Heart

A simplified structural map of the heart is shown in Fig.(12.1a). The main pumping action of the heart comes from the contraction of the left ventricle. The contraction is stimulated by an electrical pulse (called the action potential) that propagates through the conducting muscle fibres in a way that is closely analogous to the propagation of pulses in nerve fibres. The pulses ultimately derive from the “sinus node”, a small, oscillatory region on the wall of the right atrium. They spread through the atrium, and via specialized conduction fibres known as Purkinje fibres to the atrioventricular (A-V) node. (Purkinje fibres transport the pulses at an enhanced speed over the regular muscle fibres, but themselves do not contract significantly.) The ventricle is in turn stimulated from the A-V node. The signal is distributed from here via more Purkinje fibres to the ventricle wall muscle, and then through the muscle itself. The time for the electrical signal to reach the various parts of the heart is shown in Fig.(12.1b). As the signal propagates through the muscle, the fibres contract. The coherent contraction causes the volume of the ventricle cavity to decrease, and blood is pumped out of the ventricle and around the body.

A cross section of the ventricles, taken at the equator or largest section, is shown in Fig.(12.1c). The conical region of the wall of the left ventricle with the topology of a cylinder (and therefore known by this name) provides a large proportion of the pumping force.

The heart wall muscle is made up of muscle fibres that at each point are aligned predominantly along a particular direction. The fibres are however interconnected, Fig.(12.1d), so that coarse graining this structure gives a *three* dimensional conduction pathway, but with uniaxial anisotropy—enhanced conduction along the mean fibre direction compared to the transverse direction. The mean fibre direction varies spatially, and in particular rotates across the wall of the “cylinder” (i.e. from the outside to the inside). This rotation has been measured in detailed experiments, and can be understood to some degree from mechanical considerations.

### 12.2.2 The Heart as a Dynamical System

The simplest description of the dynamics of the heart ignores the complicated spatial aspects and concentrates on the empirical properties of the heart action potential. The electrical voltage of a single period is made up of four parts (see Fig. 12.2): a rapid depolarization when the voltage changes from its resting value around  $-85mV$  to about  $+15mV$ ; a rapid drop to a plateau at around  $-10mV$ ;

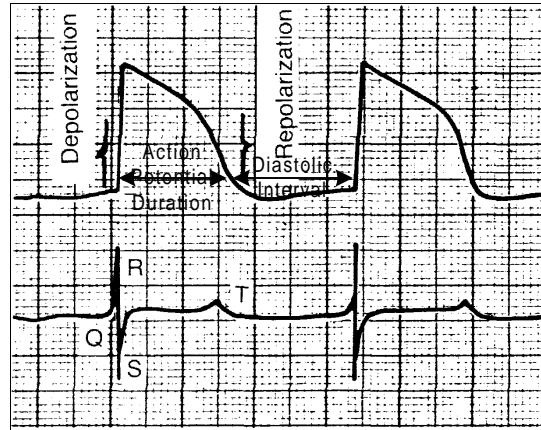


Figure 12.2: Top: action potential in a ventricular muscle fibre, showing rapid depolarization and slower repolarization. The "action potential duration" and diastolic interval" are indicated for a choice of threshold value. Bottom: corresponding ECG trace.

a repolarization to the resting period that is rapid but not as sharp as the initial depolarization; and finally a return to the resting voltage until the next depolarization. The time variation at each point has strong analogies to the "relaxation oscillations" of the van der Pohl oscillator. Indeed in 1928 van der Pohl and van der Mark proposed a simple circuit with a neon tube nonlinear element, described by the equation we now call the van der Pohl equation, as a simple model of the beating of the heart.

During the resting time subsequent to an action potential pulse there is a refractory period in which the medium is less sensitive to a following voltage stimulus, and the *duration* and *size* of a subsequent action potential pulse (for a given stimulus size) depends on the delay. A simple characterization of this is given by the "action potential restitution curve", which plots the action potential duration against the prior diastolic interval, i.e. the time the depolarization lasts against the length of time previously spent in the depolarized state. To get a quantitative measure the times are defined at some chosen reference level (e.g. 85% depolarization). Alternatively the size of the action potential is plotted against the diastolic interval.

We can use the action potential restitution curve to indicate the possibility of complex dynamics in the heart. Consider the response of a piece of heart muscle

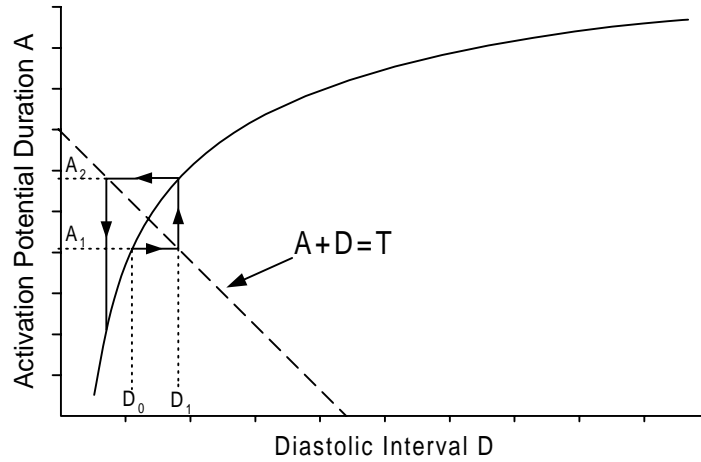


Figure 12.3: Period Doubling in the Heart. The full curve is the “action potential restitution” curve giving the length of the action potential  $A$  following a diastolic interval  $D$ . Since the onset of the next action potential is determined by the external pulsing at period  $T$  the  $n$ th diastolic interval  $D_n$  is determined by  $T - A_n$  (the horizontal arrows to the dashed line  $A + D = T$  in the plot). The next action potential duration  $A_{n+1}$  is determined by the full curve (vertical arrows).

to a periodic stimulation with period  $T$ . Then the action potential duration for the  $n$ th pulse  $A_n$  and the subsequent diastolic interval  $D_n$  satisfy

$$A_n + D_n = T. \quad (12.1)$$

In addition if we ignore memory effects, the  $n$ th action potential duration depends only on the preceding diastolic interval through the restitution curve  $R$  so that

$$A_{n+1} = R(D_n) \quad (12.2)$$

$$D_n = T - A_n. \quad (12.3)$$

These two relationships give a simple “one dimensional map” for the discrete time dynamics. Note that instead of the usual “diagonal line” step-tread type construction, successive input values are given by reflection in the line of slope  $-1$  and intercept  $T$ .

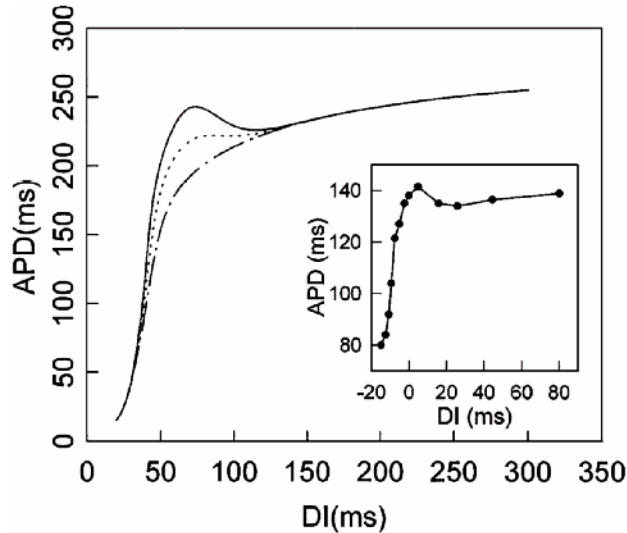


Figure 12.4: Non-monotonic action potential restitution curves: inset—experiments of Watanabe et al. [15]; main curves—from theoretical models of the action potential with three different choices of parameters (from Qu et al. [16])

The dynamics can easily be reconstructed graphically as shown in Fig.(12.3). The intersection of the line and curve gives the periodic solution  $A_n = A^*$  corresponding to a regular heart beat

$$A^* = R(T - A^*). \quad (12.4)$$

However if the slope of the restitution curve is greater than unity this solution is seen to be *unstable*, and the pulse train settles down to alternating long and short pulses. Note that the fixed point, and its stability, may be tuned by varying the period  $T$  of the external stimulus.

If the restitution curve is more complex, with a maximum as in Fig.(12.4), the dynamics may even become chaotic through an infinite sequence of period doubling bifurcations. The most direct application of this simple theory is to controlled laboratory experiments where *in vitro* pieces of cardiac Purkinje fibres [17] or pieces dog ventricle muscle [15] are stimulated by a periodic sequence of applied electrical pulses. These experiments do indeed show transitions to complex dynamics. For example, in Fig.(12.5) the complexity of the dynamics increases, showing period doubling, locking, and irregular dynamics (ID), as the period of

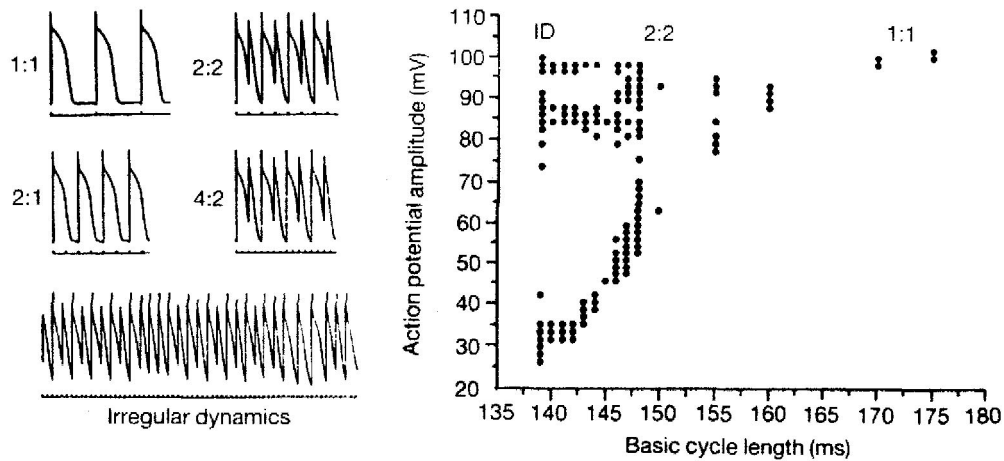


Figure 12.5: Pulse sequences and bifurcation diagram for experiments on Purkinje fibres from a sheep heart. (From Chialvo et al. [17])

the applied pulse sequence is decreased leading to a steeper slope of the action potential restitution curve.

Presumably in the healthy heart the period of pulses from the sinus node pacemaker does not take the heart into the dangerous, unstable regime. However the electrical pathway of the heart muscle may become re-entrant. This may occur either because of a pathology in the structure of the heart (e.g. the path surrounding a portion of the muscle killed by oxygen deprivation) or because of the spontaneous formation of spiral-like wave structures, where the waves rotate about a central core, see Fig.(12.6). In these cases the period of the stimulation is given by the circulation time of the waves, usually shorter than the regular beat period. Although the situation is certainly more complicated now, since there is no longer a fixed external stimulation, we might use the preceding discussion to motivate the idea that the periodic wave structure may break down, first by a period doubling or alternans, and then perhaps further to a disordered state. Simulations of models involving these types of spatial structures [20], do indeed see this type of breakdown of the regular wave structure.

It is now believed that the state of ventricular fibrillation is indeed quite likely to be a state in which the heart dynamics is chaotic, but the spatial structure is also complex or disordered (i.e. the dynamics is high dimensional). The simple global description in terms of the low dimensional chaos of a single propagating pulse is

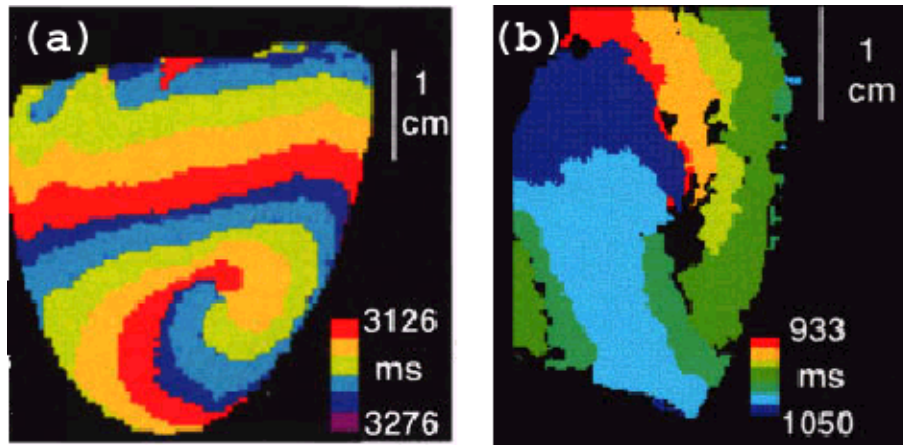


Figure 12.6: Spiral wave structure in the heart: (a) numerical simulations of a model of the electrical propagation in a realistic heart geometry (b) experiments on *in vitro* rabbit heart [18]. The coloring indicates the *time* at which an action potential pulse reaches that region of the heart, and so gives a picture of the propagating pulse. (Pictures taken from Jalife et al. [19].)

probably not sufficient, although the approach may well be useful in understanding the initial breakdown of the periodically beating structures [21]. You can find some simulations of vastly simplified models showing different types of spatial structure under the “Patterns and Spatiotemporal Dynamics” [link](#) on my website [22].

February 21, 2000

# Bibliography

- [1] G. Ahlers, Phys. Rev. Lett. **33**, 1185 (1974)
- [2] J.P. Gollub and H.L. Swinney, Phys. Rev. Lett. **35**, 927 (1975)
- [3] H.S. Greenside, M.C. Cross and W.M. Coughran, Phys. Rev. Lett. **60**, 2269 (1988)
- [4] M. Dubois and P. Bergé, J. de Physique **42**, 167 (1981)
- [5] B. Malraison, P. Atten, P. Bergé, and M. Dubois, J. de Physique Lett. **44**, L897 (1983)
- [6] J.-C. Roux, R.H. Simoyi, and H.L. Swinney, Physica **8D**, 257 (1983)
- [7] R.H. Simoyi, A. Wolf and H.L. Swinney, Phys. Rev. Lett. **49**, 245 (1982)
- [8] J.A. Glazier, M.H. Jensen, A. Libchaber, and J. Stavans, Phys. Rev. **A34**, 1621 (1986)
- [9] J.A. Glazier, L.P. Kadanoff, A. Libchaber, I. Procaccia and J. Stavans, Phys. Rev. Lett. **55**, 2798 (1985)
- [10] A. Wolf, J.B. Swift, H.L. Swinney, and J.A. Vastano, Physica **16D**, 285 (1985)
- [11] P. Grassberger and I. Procaccia, Phys. Rev. **A28**, 2591 (1983)
- [12] R. Hegger, H. Kantz, and T. Schreiber, Chaos **9**, 413 (1999)
- [13] A.C. Guyton and J.E. Hall, *Textbook of Medical Physiology* (Saunders, Philadelphia 1996)
- [14] C.E. Thomas, Am. J. Anatomy **101**, 17 (1957)

- [15] M. Watanabe, N.F. Otani, and R.F. Gilmour, *Circ. Res.* **76**, 915 (1995)
- [16] Z. Qu, J.N. Weiss, and A. Garfinkel, *Phys. Rev. Lett.* **78**, 1387 (1997)
- [17] D.R Chialvo, R.F. Gilmour, and J. Jalife, *Nature* **343**, 653 (1990)
- [18] J. Jalife and R. Gray, *Acta. Physiol. Scand.* **157**, 123(1996)
- [19] J. Jalife, R.A. Gray, G.E. Morley, and J.M. Davidenko, *Chaos* **8**, 79 (1998)
- [20] M. Courtemanche, L. Glass, and J.P. Keener, *Phys. Rev. Lett.* **70**, 2182 (1993)
- [21] A. Karma, *Chaos* **4**, 461 (1994)
- [22] M.C. Cross, [website](http://www.cmp.caltech.edu/~mcc/): <http://www.cmp.caltech.edu/~mcc/>